Clim Dyn (2015) 45:325–335
DOI 10.1007/s00382-014-2376-1

GCMs with implicit and explicit representation of cloud microphysics for simulation of extreme precipitation frequency

In-Sik Kang · Young-Min Yang · Wei-Kuo Tao

Received: 16 March 2014 / Accepted: 13 October 2014 / Published online: 26 October 2014

Abstract The present study aims to develop a general circulation model (GCM) with improved simulation of heavy precipitation frequency by improving the representations of cloud and rain processes. GCMs with conventional convective parameterizations produce common bias in precipitation frequency: they overestimate light precipitation and underestimate heavy precipitation with respect to observed values. This frequency shift toward light precipitation is attributed here to a lack of consideration of cloud microphysical processes related to heavy precipitation. The budget study of cloud microphysical processes using a cloud-resolving model shows that the melting of graupel and accretion of cloud water by graupel and rain water are important processes in the generation of heavy precipitation. However, those processes are not expressed explicitly in conventional GCMs with convective parameterizations. In the present study, the cloud microphysics is modified to allow its implementation into a GCM with a horizontal resolution of 50 km. The newly developed GCM, which includes explicit cloud microphysics, produces more heavy precipitation and less light precipitation than conventional GCMs, thus simulating a precipitation frequency that is closer to the observed. This study demonstrates that the GCM requires a full representation of cloud microphysics to simulate the extreme precipitation frequency realistically. It is also shown that a coarse-resolution GCM with cloud microphysics requires an additional mixing process in the lower troposphere.

Keywords Frequency of heavy precipitation · Cloud resolving model · GCM · Cold-cloud processes · Cloud microphysics

I.-S. Kang (✉)
School of Earth and Environmental Sciences, Seoul National University, Seoul 151-747, South Korea
e-mail: kang@climate.snu.ac.kr

Y.-M. Yang
International Pacific Research Center, SOEST, University of Hawaii, Honolulu, HI 96822, USA

W.-K. Tao
Mesoscale Atmospheric Processes Laboratory, NASA/Goddard Space Flight Center, Greenbelt, MD 20771, USA

1 Introduction

Extreme precipitation events often create severe sociological, ecological, and economic damage in the regions affected by such events. In recent decades, significant increasing trends have been reported in the magnitude and frequency of heavy precipitation (O'Gorman and Schneider 2009; Scoccimarro et al. 2013), and further increase over the next century has been projected by a number of GCM simulations under global warming scenarios (Allan et al. 2010; Kharin et al. 2007; Lau et al. 2013; Liu et al. 2012; Min et al. 2011; Sun et al. 2012 and others). However, uncertainties in these future projections have also been reported repeatedly, primarily because current climate models commonly underestimate the occurrence of intense precipitation and fail to simulate extreme precipitation events (Durman et al. 2001; Boyle and Klein 2010; Li et al. 2011a). Thus, to obtain a robust projection of extreme precipitation frequency, it may be necessary to develop a GCM that can simulate the statistics of the extreme precipitation of the present climate reasonably well.

Several studies have demonstrated that GCMs with conventional convective parameterizations tend to overestimate light rain and cannot reproduce extreme precipitation above a certain threshold value (Dai 2006; Sun et al. 2006).

Two primary reasons have been suggested for this frequency shift of GCM rainfall intensity toward light precipitation. The first one is the coarse horizontal resolutions of convectional GCMs. Chen and Knutson (2008) and Wehner et al. (2010) showed that GCMs with low horizontal resolution (i.e., grid size of the order of 100 km) cannot simulate severely heavy precipitation, and Boyle and Klein (2010) demonstrated that increasing the horizontal resolution of GCMs yields more realistic spatial patterns and precipitation probability distributions over most continental regions. Conversely, Li et al. (2011b) demonstrated in ideal experiments that the horizontal resolution of GCMs does not affect the frequency of heavy precipitation, based on the fact that heavy precipitation statistics remained unchanged in response to increases in spectral truncation above T170. In fact, Iorio et al. (2004) showed that a GCM with a horizontal resolution of T239 still underestimates the frequency of heavy precipitation.

The second reason for the frequency shift is poor representations of moist physical processes in convectional GCMs. It is well known that arbitrary setting of cloud tops of ensemble clouds in the Arakawa–Schubert scheme results in frequent occurrence of deep convective clouds; this leads to less pronounced accumulation of convective instability and therefore less occurrence of heavy precipitation. To remedy this problem, several triggering mechanisms have been introduced into Arakawa–Schubert type convective parameterizations, including the Tokioka trigger (Tokioka 1988; Lee et al. 2001, 2003) and threshold relative humidity (Wang and Schlesinger 1999). Furthermore, several studies have demonstrated that the simulation of precipitation amount and distribution is sensitive to the entrainment and detrainment equations in the convective parameterization (Kim and Kang 2012; Gregory 2001). However, the parameters involved in convective triggers and entrainment/detrainment equations are very uncertain and difficult to be determined by observation, and some phenomena such as the Madden–Julian oscillation can be improved by introducing the convective triggers, yet this often involves sacrificing accuracy in other phenomena such as climatology (Kim et al. 2011; Mapes and Neale 2011). The closure of cumulus parameterization has also been demonstrated to be an important factor influencing the frequency of simulated convective precipitation (Pan and Randall 1998; Khairoutdinov and Randall 2003; Lin et al. 2000; Scinocca and McFarlane 2004; Lorant et al. 2006). In particular, Lorant et al. (2006) introduced a prognostic closure and demonstrated that it produces more intense convective precipitation than that of a closure using convective available potential energy (CAPE). However, they found that changes in the frequency of convective precipitation are offset by opposite changes in the frequency of large-scale condensation, resulting in little improvement in simulation of the frequency of total precipitation. In consistent to the study by Lorant et al., Li et al. (2011b) also demonstrated that the improvement of convective parameterization in the conventional GCM framework may have a limited impact on the frequency of total precipitation.

Recently, explicit representation of the moist physical processes of cloud and rain has been suggested as a promising alternative to the parameterizations and may improve the simulation of the frequency of heavy precipitation in a given model. Wilcox and Donner (2007) examined the frequency of heavy precipitation using various GCMs with different convective parameterizations and explicit representations of ice processes. They showed that an explicit representation of ice processes improves the frequency of heavy precipitation with respect to conventional parameterizations. Improvements in the simulation of the frequency of heavy precipitation using an explicit representation of cloud processes have also been reported with the GCM with a multiscale modeling framework (MMF) referred to as the "super-parameterized GCM," in which the convective parameterization and large-scale condensation are replaced by cloud-resolving model (CRM) physics. However, the MMF does not express the CRM physics explicitly with GCM state variables; rather, it embeds the CRMs in each grid box of a GCM (Iorio et al. 2004; DeMott et al. 2007; Li et al. 2012). DeMott et al. (2007) demonstrated that a GCM with the super-parameterization was able to simulate the observed precipitation processes more reasonably than conventional GCMs by showing that the super-parameterized GCM simulates a gradual increase in low-level relative humidity prior to rainfall, in agreement with observations (DeMott et al. 2007). Conversely, in conventional GCMs, precipitation reacts more or less simultaneously to large-scale thermal instability owing to the quasi-steady state assumption of the convective parameterization. Li et al. (2012) revealed that improvements in heavy precipitation simulated by the super-parameterized GCM were due primarily to increases in cloud water path and cloud condensation, which are not included or poorly expressed in conventional convective parameterizations.

It has been suggested that the MMF method used by the super-parameterization is an intermediate way of incorporating the cloud microphysics in GCMs, because the MMF does not allow the interaction between the clouds in adjacent GCM grids and uses an arbitrary cyclic boundary condition within a single grid box by embedding the CRM in each grid box of the GCM. In the present study, on the other hand, the GCM cloud and rain processes are represented by the CRM physics. In other words, the CRM domain is extended to the global domain and the CRM processes are computed using GCM state variables. This approach may require a very high horizontal resolution (e.g., a few km) and has been adopted previously in the

nonhydrostatic icosahedral atmospheric model described by Satoh et al. (2005). However, the horizontal resolution of the present model is ~50 km; accordingly, the ability of this model to express CRM processes is limited. Therefore, in the present study, we modified some of parameters in the CRM physics that are sensitive to horizontal resolution. Additionally, the subgrid-scale mixing with various types of diffusion formula is considered and included in the present GCM, since a coarse-resolution model with the CRM physics results in relatively small vertical mixing owing to a lack of representation of subgrid-scale convective mixing.

Here, we describe the development of a GCM with a horizontal resolution of 50 km that incorporates a representation of cloud microphysics and demonstrate that this new model improves the simulation of the frequency of heavy precipitation. Section 2 describes the models utilized and their simulations. Section 3 investigates the dominant cloud microphysical processes for heavy precipitation by using the CRM simulations. Section 4 describes the GCM incorporating a modified representation of CRM physics. The effects of cloud microphysics on the frequency of heavy precipitation are examined by comparing the GCM simulations with cloud microphysics and those with a conventional convective parameterization. Finally, a summary and discussion are presented in Sect. 5.

2 Models

The models used in the present study include a cloud-resolving model (CRM) and a GCM for the implementation of the CRM physics. The CRM adopted is the Goddard Cumulus Ensemble Model developed at the Goddard Space Flight Center of the National Aeronautic Space Administration (Tao et al. 2003). The CRM includes a dynamical core, microphysics, radiation, surface flux, and a subgrid-scale turbulence scheme. The dynamical core uses compressible equations (Klemp and Wilhelmson 1978) with periodic lateral boundary conditions. The cloud microphysics representation includes the Kessler-type two-category liquid water scheme and the three-category ice-phase scheme, developed mainly by Lin et al. (1983). We use a two-dimensional version of the model, where the domain size is 256 km in the x-axis and the horizontal grid size is 1 km. The vertical resolution is about 80 m near the surface and increases gradually with height to reach approximately 700 m near the 10 km level.

The atmospheric general circulation model (AGCM) used in this study is a Seoul National University AGCM. The model has a finite-volume dynamical core with a hybrid sigma-pressure vertical coordinate system and is represented at a horizontal resolution of 50 km with 20 vertical levels. The deep convection scheme adopted is

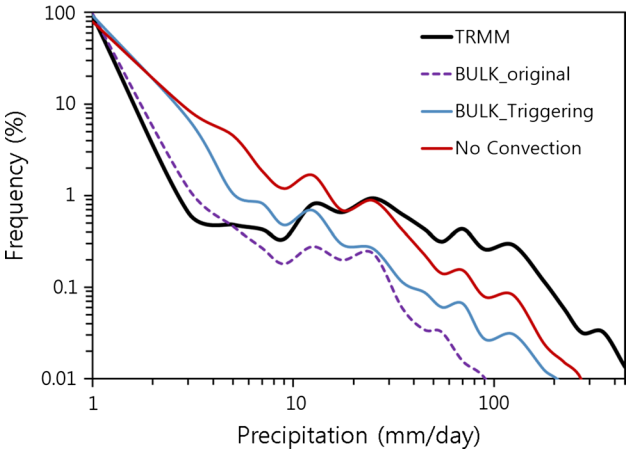

Fig. 1 Frequency distribution of three-hourly precipitation as a function of precipitation intensity from TRMM (*black*), the GCM with the BULK scheme with (*solid blue line*) and without (*dashed purple line*) triggering mechanism, and the GCM without convective precipitation (*solid red line*). The bin size is 1 mm day^{-1} for 0–60 mm day^{-1} of precipitation and increases gradually to 20 mm day^{-1} at 200 mm day^{-1}. *Note* the logarithmic scale

a mass flux scheme developed by Kim and Kang (2012), which is basically similar to the bulk mass flux scheme of Tiedtke (1989). The differences between the two schemes are in the entrainment and detrainment equations and mass flux closure. The large-scale condensation scheme, based on Le Treut and Li (1991), converts the relative humidity exceeding 75 % to precipitation with a relaxation time scale of 3600 s. The shallow convection is represented by a diffusion-type convection scheme of Tiedtke (1984); this scheme does not produce precipitation and is turned off when the deep convection occurs. The boundary layer scheme is a nonlocal diffusion scheme described by Holtslag and Boville (1993), and radiation processes are parameterized by the two-stream k-distribution scheme implemented by Nakajima et al. (1995). The land surface processes are represented by the land surface model of Bonan (1996), developed at the National Center for Atmospheric Research. A detailed description of physical parameterizations in the AGCM can be found in Kim and Kang (2012).

The model of Kim and Kang (2012) exhibits a limited ability to simulate extreme precipitation, particularly three-hourly mean precipitation >120 mm day^{-1} (Fig. 1). Figure 1 illustrates the frequency of three-hourly precipitation over the tropics (30°S–30°N). Different precipitation intervals are used to obtain Fig. 1; the bin size is 1 mm day^{-1} for 0–60 mm day^{-1} of precipitation and increases gradually to 20 mm day^{-1} at 200 mm day^{-1}. Here, the GCM results are based on a 4-year simulation with the climatological varying SST boundary condition prescribed. The Tropical Rainfall Measuring Mission (TRMM, Huffman et al. 2007)

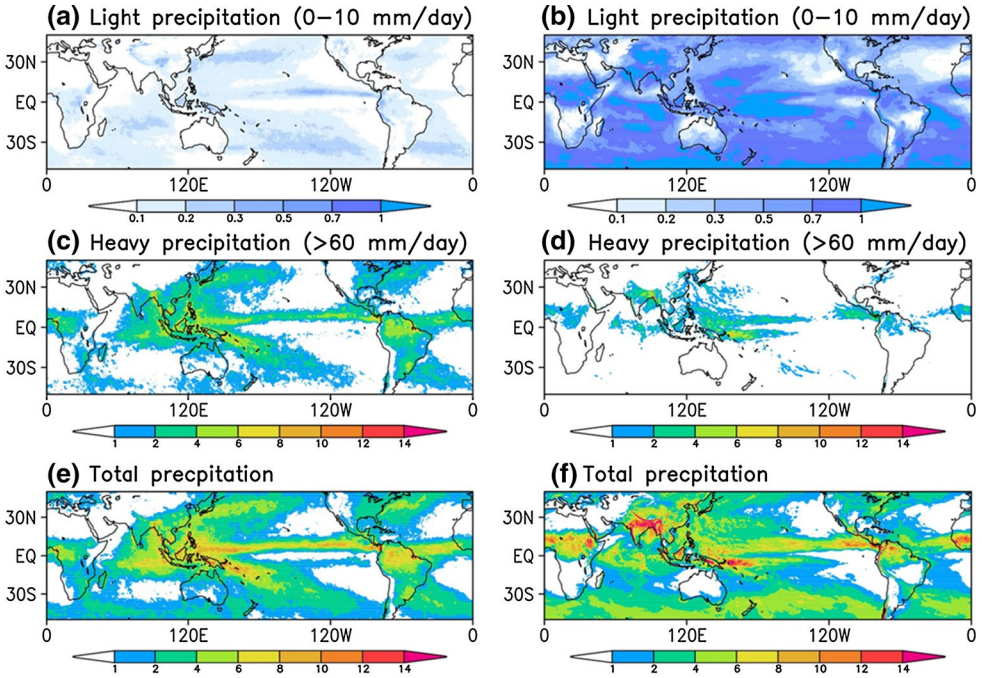

Fig. 2 Spatial distribution of **a**, **b** light (<10 mm day^{-1}; *upper*), **c**, **d** heavy (>60 mm day^{-1}; *middle*), and **e**, **f** total precipitation (*lower*) of the TRMM and the GCM with the BULK scheme. Three-hourly precipitation data are used for classifying the light and heavy precipitation

precipitation data for the 10 years of 1998–2007 is used for the observed counterpart. It is noted that the horizontal grid system of original TRMM data, which has a resolution of 25 km in the tropics, was converted to the model grid system with the 50 km resolution by using an area-weighted method. It is clear that the model overestimates and underestimates light and heavy rain, respectively, compared to the observations. To simulate heavy precipitation more frequently, a triggering mechanism is implemented in the convection scheme by adding a minimum cloud-base mass flux. This triggering mechanism suppresses convection when the cloud-base vertical velocity is less than a certain value. We have tested the values from 0.1 to 0.3 m s^{-1} and adopted a value of 0.2 m s^{-1} based on consideration of the simulated precipitation characteristics, particularly the climatology and precipitation frequency. The model with the triggering mechanism is used as a standard AGCM in the present study. The standard AGCM produced more frequent precipitation across all intensity spectrums than those of the model without the triggering mechanism (Fig. 1). However, the AGCM still underestimates the frequency of heavy precipitation compared to the observations and this model has only limited success in the simulation of extreme precipitation. It does not produce precipitation of more than 220 mm day^{-1}. The horizontal distributions of the simulated light and heavy precipitation are also examined by comparing them to the observed counterparts. Figure 2a, c, e, illustrate the spatial distributions of light (i.e., three-hourly mean precipitation <10 mm day^{-1}), heavy (i.e., three-hourly precipitation >60 mm day^{-1}), and the total precipitation, respectively, obtained from the TRMM data. Similarly, Fig. 2b, d, and f illustrate the corresponding simulated distributions. The TRMM data indicate that the 10-year mean precipitation (Fig. 2e) is composed primarily of heavy precipitation (Fig. 2c), particularly over tropical rainy regions such as the Inter-Tropical Convergence Zone (ITCZ) and the western Pacific. In these rainy regions, light precipitation (Fig. 2a) is also relatively abundant compared to other tropical regions. In contrast, the simulated light precipitation is overestimated with respect to the observations and exhibits an almost uniform distribution throughout the tropics (Fig. 2b), whereas heavy precipitation is underestimated, particularly in the western Pacific (Fig. 2d). As a result, the mean total precipitation (Fig. 2f) exhibits a large bias in the western Pacific. Moreover, the rain band observed in the western Pacific is shifted to the south in the simulated precipitation pattern.

3 Rain processes in a cloud-resolving model

The biases in simulated precipitation characteristics shown in the previous section may be a result of the poor representation of moist physical processes (e.g., convective, cloud, and rain processes) in the model. The parameterizations of rain processes in the AGCM used here are relatively simple, with just two rain species (i.e., water and ice), although actual rain processes are complex and include interactions between various cloud and rain species. The CRM was developed to mimic the observed processes of cloud and rain and incorporates five cloud and rain species: cloud water, cloud ice, rain water, graupel, and snow (Tao et al. 2003; Lin et al. 1983).

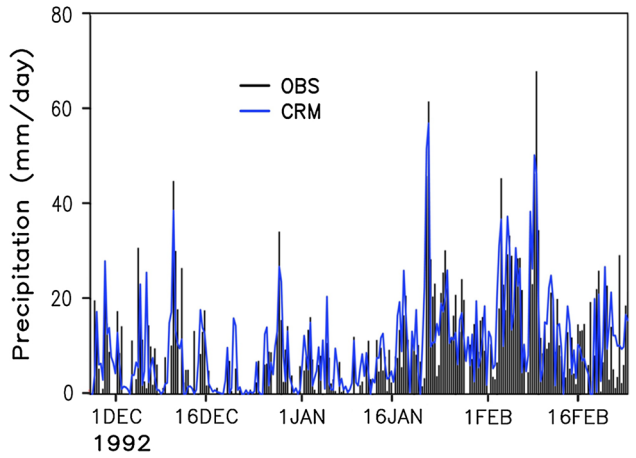

Fig. 3 Six-hour mean precipitation rates (mm day^{-1}) averaged over the model domain from CRM (*blue line*) and TOGA COARE observations (*black bar*) for boreal winter

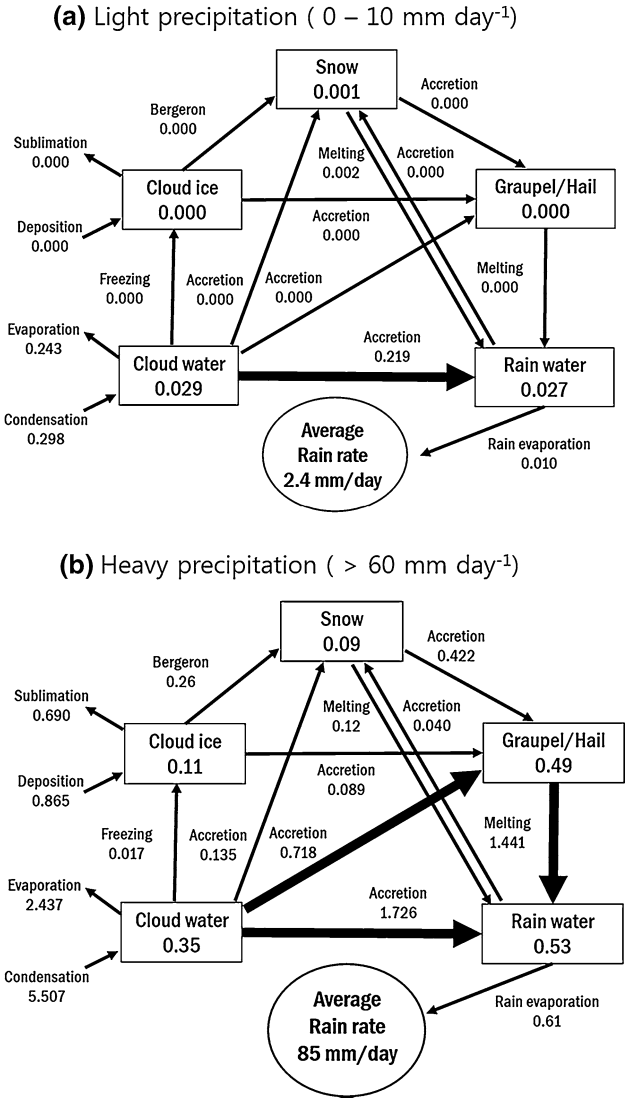

Fig. 4 Budget of cloud microphysical processes of the CRM for **a** light and **b** heavy precipitation. Thick (*thin*) arrow represents major (*minor*) microphysical processes

Here, we examine the rain processes using the CRM and identify the important processes that are not represented in the AGCM, particularly those related to heavy precipitation.

The CRM is integrated from 28 November 1992 to 31 January 1993, which corresponds to the duration of the Tropical Ocean and Global Atmosphere Coupled Ocean–Atmosphere Response Experiment (TOGA COARE; Webster and Lukas 1992). The initial conditions and forcing data are obtained from the Global Energy and Water Cycle Experiment (GEWEX) Cloud System Study (Ciesielski et al. 2003). The simulated six-hourly mean precipitation averaged over the model domain of 2°S–4°S and 155°E–158°E is compared with the corresponding data from the TOGA COARE. Figure 3 demonstrates that the time series of simulated precipitation mimics its observed counterpart, with a correlation coefficient of 0.73. In particular, heavy precipitation events are simulated reasonably well, indicating that the CRM has a capacity to simulate the observed heavy precipitation events. Using the CRM simulation data, we examine the budget of the microphysics of precipitation processes to identify important cloud and rain processes for light and heavy precipitation separately. Here, the light and heavy precipitation are defined as precipitation <10 mm day^{-1} and more than 60 mm day^{-1}, respectively. As seen in Fig. 4a, the rain water involved in light precipitation originates from cloud water produced by the condensation of water vapor. For light precipitation, the vertical velocity is relatively weak (not shown), and the water vapor confined in the warm lower troposphere is converted to the cloud and rain water. On the other hand, for the heavy precipitation associated with strong vertical motion, the water vapor can be transported to the cold upper-troposphere, and therefore the rain water is originated not only from the cloud water in the lower troposphere but also from ice phases of cloud water such as ice, snow, and graupel in the middle and upper troposphere (Fig. 4b). In particular, Graupel is produced primarily through the accretion of cloud water and is converted to rain water by melting processes. Some graupel is produced by the accretion of snow. In the GCM, the rain water is sourced primarily from cloud water, with a small portion originating from cloud ice. Therefore, the rain processes of the GCM mimic the microphysical processes involved in the generation of light precipitation; however, the GCM does not incorporate major rain processes, such as the growth of graupel and its melting processes, for heavy precipitation. In other words, the GCM must include the microphysical processes associated with ice phases of cloud water (e.g., snow and graupel) to be able to simulate heavy precipitation realistically.

The importance of the role of graupel in simulating heavy precipitation is clearly demonstrated by Fig. 5a, which illustrates the relationship between rainfall intensity and the amount of graupel integrated vertically within the cloud column. This figure indicates that the contribution of graupel is negligible for light rain (i.e., <10 mm day^{-1}) but increases almost linearly with increasing rain intensity up to 200 mm day^{-1} and appears to saturate for the heavy precipitation more than 200 mm day^{-1}. A similar relationship is evident between rainfall intensity and the accretion of cloud water by graupel (Fig. 5b). The two panels of Fig. 5 demonstrate clearly that the accretion of cloud water is an important source of graupel and that large amounts of graupel are required to produce heavy precipitation. However, both accretion and the input of graupel are negligible for light precipitation (i.e., up to 10 mm day^{-1}); accordingly, light rain is produced primarily by warm rain processes without ice species, as demonstrated by Fig. 4a. The vertical profiles of various cloud and rain species of the CRM for the light and heavy precipitation cases are presented in Fig. 6a, b, respectively. As expected, for the light precipitation case (Fig. 6a), cloud and rain water are confined to the lower troposphere and no water or ice species exist in the middle and upper levels. In contrast, for the heavy precipitation case (Fig. 6b), abundant graupel appears in the middle and upper levels (i.e., above 700 hPa). Even in the upper levels, where air temperature is typically well below freezing level, graupel is more abundant than cloud ice. The upper-level graupel appears not to be generated locally; rather, it appears to be transported from the middle level of the troposphere by uplift of deep convection. Figure 6b also shows that in the upper-troposphere, cloud ice generated locally by decomposition is less abundant than graupel. Abundant cloud and rain water exist in the lower level, whose maximum appears below 600 hPa. It is noted that the most pronounced differences between light and heavy precipitation can be found in the vertical distributions of graupel and cloud ice. The corresponding vertical distributions of the hydrometeors of the GCM averaged over the TOGA COARE region are illustrated in Fig. 6c, d for light and heavy precipitation, respectively. It is notable that the hydrometeors in the present GCM are confined to cloud water and cloud ice. As seen in Fig. 6c, GCM light rain originates not only from cloud water in the lower layer but also cloud ice in the deep cloud. This confirms that the GCM overestimates light rain owing to too-frequent generation of deep convection. For heavy precipitation, the GCM rainfall results primarily from cloud water, which is much more abundant than that of the CRM simulation. Cloud ice occurs above 400 hPa, which is higher than that of the CRM, and the cloud ice content is also more abundant in the GCM than that in the CRM. We attribute the biases in the simulated profiles of cloud water and ice to the lack of

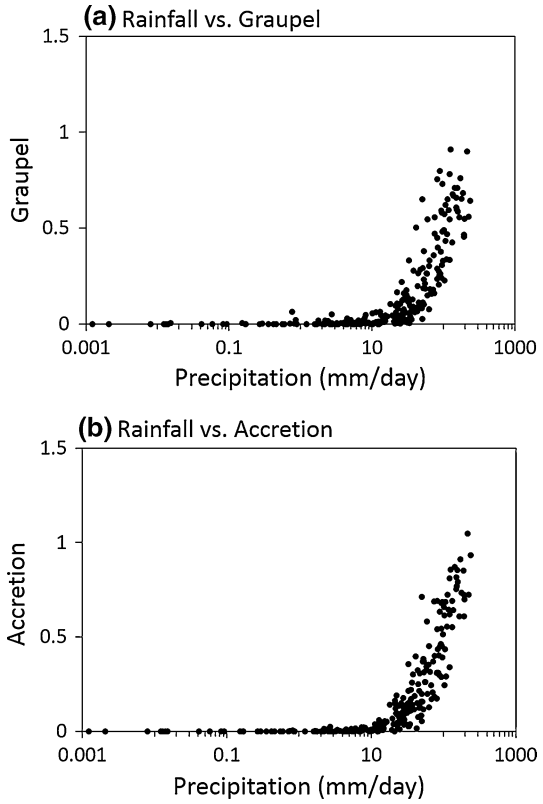

Fig. 5 Scatter plots of **a** graupel (kg m^{-2}) and precipitation (mm day^{-1}) and **b** accretion of cloud water by graupel (kg m^{-2} s^{-1}) and precipitation in the CRM simulation. Both graupel and accretion are averaged vertically within the cloud column

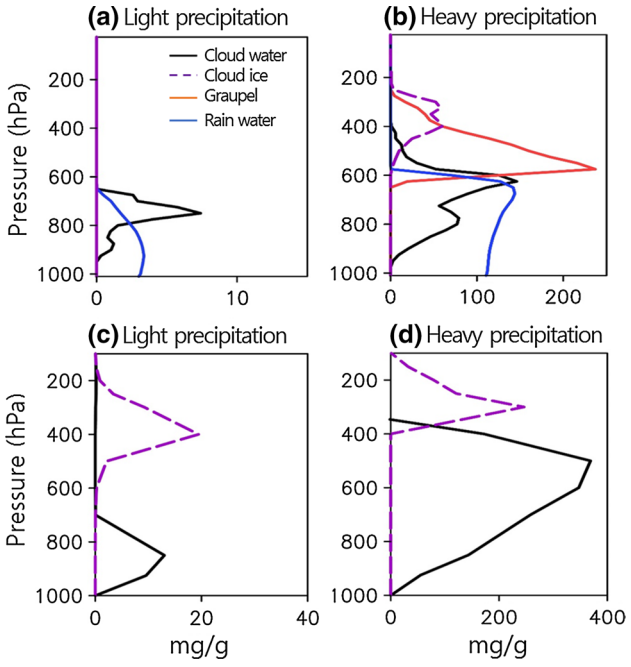

Fig. 6 Composite of cloud hydrometeors (g kg^{-1}) obtained using **a**, **b** the CRM and **c**, **d** the GCM with parameterizations for light (*left*) and heavy (*right*) precipitation events

consideration of graupel and snow in the GCM. Thus, these results indicate that a fuller consideration of microphysics may be required to improve the simulation of cloud and precipitation characteristics.

4 AGCM with cloud microphysics

The previous section demonstrated that the precipitation processes considered in the GCM are too simple to simulate the heavy precipitation reasonably well. In particular, the ice phases of hydrometeors, particularly graupel, must be included and their interactions with cloud water should be represented in the GCM. Here, we developed a GCM incorporating the full cloud microphysics used in the CRM. Thus, in this GCM, two precipitation processes (convective parameterization and large-scale condensation) are removed and replaced with the CRM cloud microphysics. Although GCM state variables with a coarse resolution (i.e., 50 km) may be unsuitable for the calculation of cloud microphysics, the simulated mean precipitation is not unrealistic and its characteristics appear to be not worse than those of the standard GCM with the parameterizations (not shown). It is noted that the simulated precipitation intensity is relatively weak compared to the TRMM precipitation in the tropical wet regions, particularly during boreal summer. We identified the condensation criteria in the microphysics as an important source of the bias: in the CRM, condensation occurs when the air is saturated, however in the GCM with a coarse resolution of 50 km, saturation is occurred less frequently and thus less condensation occurs. To remedy this problem, we replaced the condensation criteria of the CRM microphysics with that used in the large-scale condensation scheme of the standard GCM, in that a fractional area of a grid box is saturated if the relative humidity (RH) of the grid box is >75 %. The fractional area is increased linearly from 0 at RH = 75 % to 1 at RH >100 %. We also modified the terminal velocity, which is critical for the determination of accretion and graupel amount. Owing to the relatively weak vertical motion of the coarse resolution GCM, the terminal velocities of falling rainwater and graupel are much larger than those of the CRM; accordingly, the accretion process is weaker and the large cloud droplets that typically produce heavy precipitation are formed less frequently. Therefore, we reduce the constant in the terminal velocity formula, which controls the magnitude of terminal velocity, by 50 %. The two modifications are incorporated into the cloud microphysics of the GCM, and the GCM with the modified microphysics is integrated for 2 years. It is also noted that the time scales of cloud microphysical processes are much shorter than the advective time scale of 50 km model, and therefore the time intervals of calculating the cloud microphysics and GCM

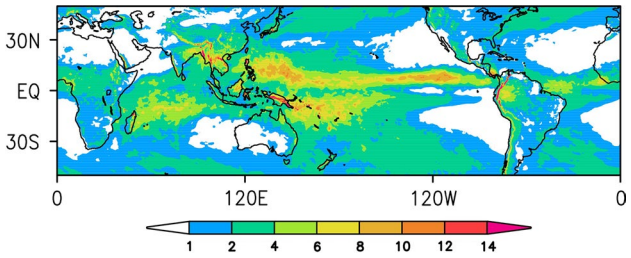

Fig. 7 Two-year mean precipitation simulated by the GCM with modified microphysics

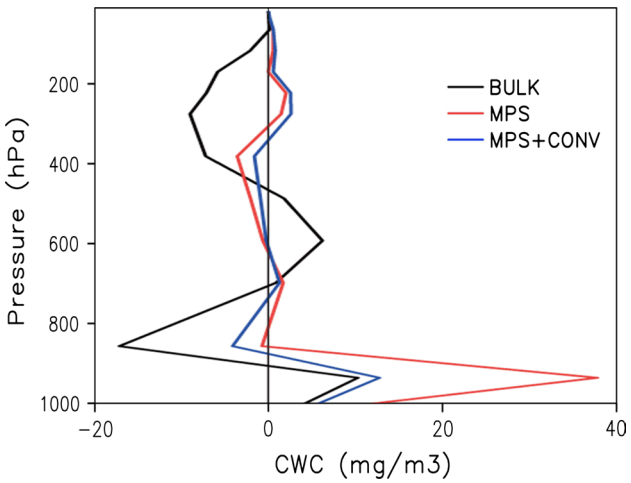

Fig. 8 Bias in annual mean cloud water content (CWC; cloud water + cloud ice) of a GCM with parameterizations (*black*), a GCM with modified microphysics (*red*), and a GCM with modified microphysics and a shallow convection scheme (*blue*). The CWC values are averaged horizontally over the tropics (30°S–30°N)

tendency terms could be different. Here we used 300 s for the time interval of the cloud microphysics and 1800 s for that of the GCM. The simulated 2-year mean precipitation is shown in Fig. 7. The spatial pattern and intensity of the simulated precipitation are generally similar to those of the TRMM (Fig. 2e), although the continental precipitation intensity is weaker, particularly in the Amazon forest region, and the double ITCZ is more evident than the observed counterparts. Except in the tropical land regions, the GCM with the modified cloud microphysics appears to simulate the annual mean precipitation, which is not worse than that of the GCM with a convective parameterization shown in Fig. 2f.

The cloud water content simulated by the GCM is compared to that of the CloudSat radar observations (Su et al. 2008). Here, the horizontal mean values over the tropics (30°S–30°N) are used to obtain the vertical profiles. Figure 8 illustrates the bias in the cloud water content simulated (simulation minus observation). A similar result can also be obtained with the TRMM3A12 data. The black and

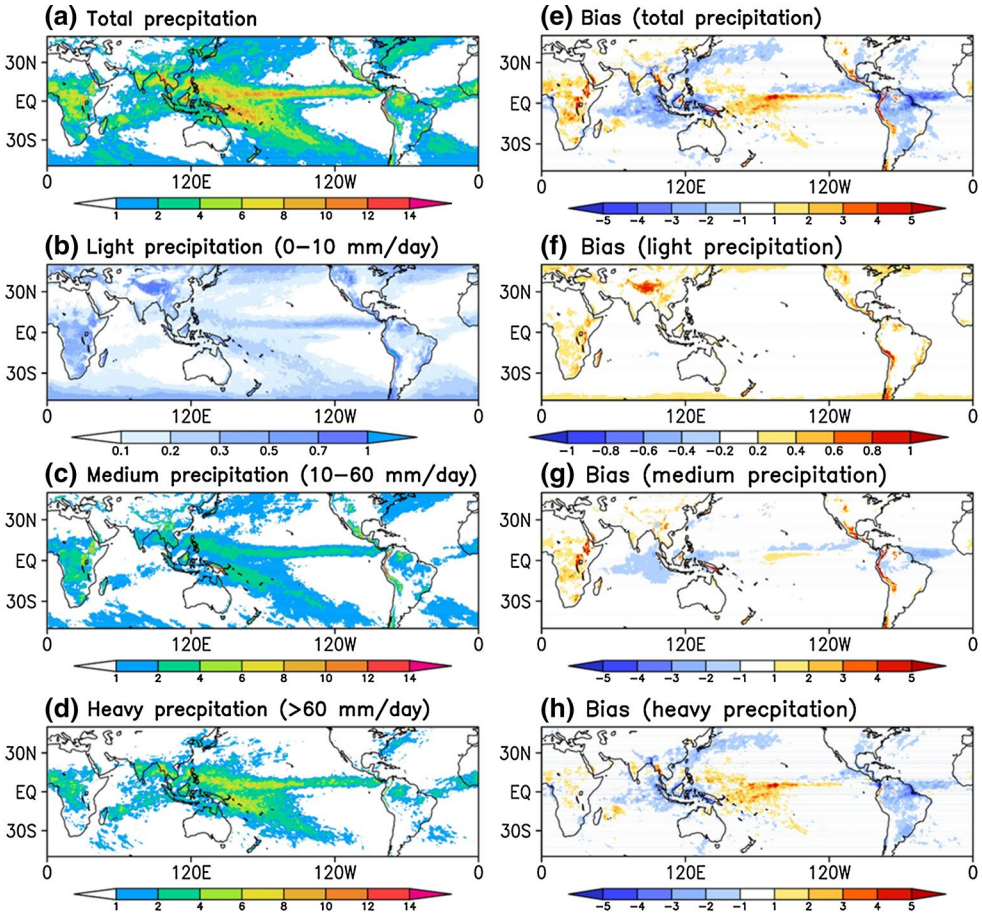

Fig. 9 Spatial distribution of **a** total, **b** light, **c** medium, and **d** heavy precipitation of the MGCM and the corresponding bias maps (**e**–**h**). Three-hourly precipitation data are used for classifying the light (<10 mm day^{-1}), medium (10–60 mm day^{-1}) and heavy (>60 mm day^{-1}) precipitation

red lines indicate the biases in the standard GCM with the parameterization and the GCM with the modified microphysics, respectively. It is clear that, when the rain processes in the standard GCM are replaced by the microphysics, the biases are much reduced in most of the vertical layers, except near the surface (i.e., below 850 hPa). The large positive biases near the surface in the GCM incorporating the microphysics are likely related to the relatively weak vertical transport of moisture from the planetary boundary layer (PBL) to the free atmosphere. This weak vertical transport occurs owing to the relatively small vertical wind associated with the coarse horizontal resolution (50 km) of the GCM compared to that of the CRM, which has a horizontal resolution of 1 km. To enhance vertical mixing near the PBL, we incorporated a diffusion-type shallow convection similar to that developed by Tiedtke (1984) into the GCM with the modified microphysics. As shown by the blue line in Fig. 8, the shallow convection actually helps mitigate the biases in the lower layer. Hereafter, the GCM with the modified microphysics and shallow convection is referred to as the modified GCM (M-GCM). The 2-year mean precipitation simulated by the M-GCM is shown in Fig. 9a. Comparison of this figure with Fig. 7 indicates that the inclusion of shallow convection reduces the excessive precipitation over the tropical eastern Pacific in both Hemispheres, more distinctively in the Southern Hemisphere, and thus the double ICTZ problem is reduced. On the other hand, the M-GCM enhances the land precipitation, particularly over the Amazon region. As a result, the M-GCM appears to simulate the precipitation pattern close to that of the TRMM shown in Fig. 2e. It is unclear and may be beyond of the scope of the present study why adding the shallow convection improves the simulation. Here we only speculate that the enhanced lower-level mixing of moisture by shallow convection reduces the precipitation in the dry subtropical High (dynamically stable) region by drying out the moisture trapped in the PBL but increases the precipitation in the wet land (thermally unstable) region where the deep convection is favored by the moisture supply from the surface. The spatial distributions of light, medium-range, and heavy precipitation are also illustrated in Fig. 9b–d, respectively. Comparison of these figures with Fig. 2 demonstrates clearly that the M-GCM reduces light precipitation and enhances heavy precipitation with respect to the standard GCM with parameterizations. Moreover, the spatial patterns produced by the M-GCM are now close to the observed (i.e., TRMM) counterparts. The medium-range precipitation (10–60 mm/day), shown in Fig. 9c, has

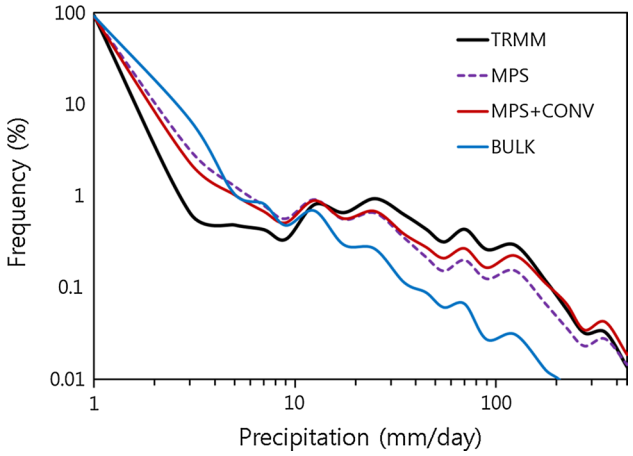

Fig. 10 Frequency distribution of three-hourly precipitation as a function of precipitation intensity from the GCM with the BULK scheme (*dashed blue line*), the GCM with modified microphysics (*solid purple line*), and the GCM with modified microphysics and a shallow convective scheme (*solid red line*). The bin size is 1 mm day^{-1} for 0–60 mm day^{-1} of precipitation and increases gradually to 20 mm day^{-1} at 200 mm day^{-1}. *Note* the logarithmic scale

a spatial distribution similar to but smaller amount than those of heavy precipitation. The corresponding bias maps, shown in Fig. 9e–h, show that regional bias of total precipitation (Fig. 9e) is mainly contributed from that of heavy precipitation (Fig. 9h). The bias of light precipitation is very small in ocean regions but is relatively big in some of land region, particularly in mountain regions. The bias of medium-range precipitation has a negative value in tropical oceans but a positive value in mountain regions.

The frequency distribution as a function of precipitation intensity is shown in Fig. 10 (the counterpart of Fig. 1). The figure incorporates the three-hourly precipitation data for the grid points in the tropics between 30°S and 30°N. The purple and red lines indicate the frequency distribution of the GCM with the modified microphysics and that of M-GCM, respectively. This figure indicates clearly that the inclusion of microphysics is important for a better simulation of precipitation for all frequencies, particularly for heavy precipitation and extreme precipitation over 200 mm day^{-1}. Furthermore, the simulated frequency is improved further when the shallow convection is added.

5 Summary and concluding remarks

The present study demonstrates that a GCM with conventional convective parameterizations tends to overestimate and underestimate light and heavy precipitation, respectively, with respect to those observed. We attribute this frequency shift toward light precipitation to the lack of representation of cloud microphysical processes related to heavy precipitation. Investigation of the water budget of cloud and rain processes using a cloud-resolving model indicates that the melting of graupel and accretion of cloud water by graupel and rain water are the dominant processes controlling heavy precipitation. Thus, warm and cold clouds should coexist in models to simulate the heavy precipitation frequency realistically. However, those processes are not expressed explicitly in conventional GCMs with convective parameterizations. Here, we describe the implementation of a modified cloud microphysics, suitable for a coarse-resolution model, in a GCM with a horizontal resolution of 50 km, and the simulated precipitation frequency is compared to those of conventional GCMs and the TRMM observations. The GCM with explicit cloud microphysics produces more heavy precipitation and less light precipitation than conventional GCMs; therefore, this new GCM simulates precipitation frequency that agrees more closely with observations. Our results demonstrate that the GCM requires a full representation of cloud microphysics to be able to simulate the observed frequency of extreme precipitation. Moreover, the coarse-resolution GCM incorporating microphysics is subject to considerable moisture bias within the PBL. This bias is due to insufficient moisture transport from the PBL to the free atmosphere owing to the relatively small vertical wind at the top of the PBL. Therefore, when the microphysics scheme is implemented, a coarse-resolution GCM requires the inclusion of an additional mixing process in the lower troposphere. Here, a shallow convective parameterization with a diffusion-type formula is included in the model for adding vertical mixing in the lower troposphere.

The spatial distribution of 2-year mean precipitation simulated by the M-GCM, which includes the modified microphysics and shallow convection, appears to be similar to that observed. However, M-GCM precipitation intensities over the tropical wet regions appear to be somewhat larger than those observed. Although a same AGCM is used for a CGCM, the precipitation pattern simulated by the CGCM differs from that of the AGCM; thus, further evaluation of the model described here should be reserved until a CGCM is developed by coupling an ocean GCM with the M-GCM. It should also be noted that there are a number of tuning parameters associated with the present representation of microphysics and shallow convection. These parameters can be tuned to improve the simulation results, although further studies are required in this regard. Also noted is that the water budget and cloud hydrometeor distribution may be sensitive to cloud microphysical parameterization. Liu et al. (2011) have shown that precipitation amount is sensitive to cloud microphysics parameterization in some specific regions, particularly mountain area. However, it is expected that the major conclusion of the present study, the importance of various ice microphysical

processes in heavy precipitation simulation, is not altered by the choice of microphysics scheme.

Acknowledgments This work was supported by a National Research Foundation of Korea (NRF) grant funded by the Korean government (MEST) (NRF-2012M1A2A2671775) and by the Brain Korea 21 Plus. Wei-Kuo Tao was supported by the NASA Precipitation Measurement Missions (PMM), the NASA Modeling, Analysis, and Prediction (MAP) Program.

References

Allan RP, Soden BJ, John VO, Ingram W, Good P (2010) Current changes in tropical precipitation. Environ Res Lett 5:1–7

Bonan GB (1996) Land surface model (LSM version 1.0) for ecological, hydrological, and atmospheric studies: technical description and user's guide. NCAR technical note NCAR/TN-417 + STR, pp 1–159

Boyle J, Klein SA (2010) Impact of horizontal resolution on climate model forecasts of tropical precipitation and diabatic heating for the TWP-ICE period. J Geohys Res 115:1–20

Chen C-T, Knutson T (2008) On the verification and comparison of extreme rainfall indices from climate models. J Clim 21:1605–1621

Ciesielski PE, Johnson RH, Haertel PT, Wang J (2003) Corrected TOGA COARE sounding humidity data: impact on diagnosed properties of convection and climate over the warm pool. J Clim 16:2370–2384

Dai A (2006) Precipitation characteristics in eighteen coupled climate models. J Clim 19:4605–4630

DeMott CA, Randall DA, Khairoutdinov M (2007) Convective precipitation variability as a tool for general circulation model analysis. J Clim 20:91–112

Durman C, Gregory J, Hassell D, Jones R, Murphy J (2001) A comparison of extreme European daily precipitation simulated by a global and a regional climate model for present and future climates. Q J R Meteorol Soc 127:1005–1015

Gregory D (2001) Estimation of entrainment rate in simple models of convective clouds. Q J R Meteorol Soc 127:53–72

Holtslag A, Boville B (1993) Local versus nonlocal boundary-layer diffusion in a global climate model. J Clim 6:1825–1842

Huffman GJ, Adler RF, Bolvin DT, Gu G, Nelkin EJ, Bowman KP, Hong Y, Stocker EF, Wolff DB (2007) The TRMM multisatellite precipitation analysis (TMPA): quasi-global, multiyear, combined-sensor precipitation estimates at fine scales. J Hydrometeorol 8:38–55

Iorio J, Duffy P, Govindasamy B, Thompson S, Khairoutdinov M, Randall D (2004) Effects of model resolution and subgrid-scale physics on the simulation of precipitation in the continental United States. Clim Dyn 23:243–258

Khairoutdinov MF, Randall DA (2003) Cloud resolving modeling of the ARM summer 1997 IOP: model formulation, results, uncertainties, and sensitivities. J Atmos Sci 60:607–625

Kharin VV, Zwiers FW, Zhang X, Hegerl GC (2007) Changes in temperature and precipitation extremes in the IPCC ensemble of global coupled model simulations. J Clim 20:1419–1444

Kim D, Kang I-S (2012) A bulk mass flux convection scheme for climate model: description and moisture sensitivity. Clim Dyn 38:411–429

Kim D, Sobel AH, Maloney ED, Frierson DM, Kang I-S (2011) A systematic relationship between intraseasonal variability and mean state bias in AGCM simulations. J Clim 24:5506–5520

Klemp JB, Wilhelmson RB (1978) The simulation of three-dimensional convective storm dynamics. J Atmos Sci 35:1070–1096

Lau WKM, Wu HT, Kim KM (2013) A canonical response of precipitation characteristics to global warming from CMIP5 models. Geophys Res Lett 40:3163–3169

Le Treut H, Li Z-X (1991) Sensitivity of an atmospheric general circulation model to prescribed SST changes: feedback effects associated with the simulation of cloud optical properties. Clim Dyn 5:175–187

Lee M-I, Kang I-S, Kim JK, Mapes BE (2001) Influence of cloud-radiation interaction on simulating tropical intraseasonal oscillation with an atmospheric general circulation model. J Geophys Res 106:14219–14233

Lee M-I, Kang I-S, Mapes BE (2003) Impacts of cumulus convection parameterization on aqua-planet AGCM simulations of tropical intraseasonal variability. J Meteorol Soc Jpn 81:963–992

Li F, Collins WD, Wehner MF, Williamson DL, Olson JG (2011a) Response of precipitation extremes to idealized global warming in an aqua-planet climate model: towards a robust projection across different horizontal resolutions. Tellus A 63:876–883

Li F, Collins WD, Wehner MF, Williamson DL, Olson JG, Algieri C (2011b) Impact of horizontal resolution on simulation of precipitation extremes in an aqua-planet version of community atmospheric model (CAM3). Tellus A 63:884–892

Li F, Rosa D, Collins WD, Wehner MF (2012) "Super-parameterization": a better way to simulate regional extreme precipitation? J Adv Model Earth Syst 4:1–10

Lin Y-L, Farley RD, Orville HD (1983) Bulk parameterization of the snow field in a cloud model. J Clim Appl Meteorol 22:1065–1092

Lin X, Randall DA, Fowler LD (2000) Diurnal variability of the hydrologic cycle and radiative fluxes: comparisons between observations and a GCM. J Clim 13:4159–4179

Liu C, Ikeda K, Thompson G, Rasmussen R, Dudhia J (2011) High-resolution simulations of wintertime precipitation in the Colorado Headwaters region: sensitivity to physics parameterizations. Mon Weather Rev 139:3533–3553

Liu C, Allan RP, Huffman GJ (2012) Co-variation of temperature and precipitation in CMIP5 models and satellite observations. Geophys Res Lett 39:1–8

Lorant V, McFarlane NA, Scinocca JF (2006) Variability of precipitation intensity: sensitivity to treatment of moist convection in an RCM and a GCM. Clim Dyn 26:183–200

Mapes B, Neale R (2011) Parameterizing convective organization to escape the entrainment dilemma. J Adv Model Earth Syst 3:1–20

Min S-K, Zhang X, Zwiers FW, Hegerl GC (2011) Human contribution to more-intense precipitation extremes. Nature 470:378–381

Nakajima T, Tsukamoto M, Tsushima Y, Numaguti A (1995) Modelling of the radiative processes in an AGCM. Clim Syst Dyn Model 3:104–123

O'Gorman PA, Schneider T (2009) The physical basis for increases in precipitation extremes in simulations of 21st-century climate change. Proc Natl Acad Sci 106:14773–14777

Pan DM, Randall DD (1998) A cumulus parameterization with a prognostic closure. Q J R Meteorol Soc 124:949–981

Satoh M, Tomita H, Miura H, Iga S, Nasuno T (2005) Development of a global cloud resolving model-a multi-scale structure of tropical convections. J Earth Simul 3:11–19

Scinocca JF, McFarlane NA (2004) The variability of modeled tropical precipitation. J Atmos Sci 61:1993–2015

Scoccimarro E, Gualdi S, Zampieri M, Bellucci A, Navarra A (2013) Heavy precipitation events in a warmer climate: results from CMIP5 models. J Clim 26:7902–7911

Su H, Jiang JH, Vane DG, Stephens GL (2008) Observed vertical structure of tropical oceanic clouds sorted in large-scale regimes. Geophys Res Lett 35:1–6

Sun Y, Solomon S, Dai A, Portmann RW (2006) How often does it rain? J Clim 19:916–934

Sun F, Roderick ML, Farquhar GD (2012) Changes in the variability of global land precipitation. Geophys Res Lett 39:1–6

Tao W-K, Simpson J, Baker D, Braun S, Chou M-D, Ferrier B, Johnson D, Khain A, Lang S, Lynn B (2003) Microphysics, radiation and surface processes in the Goddard Cumulus Ensemble (GCE) model. Meteorol Atmos Phys 82:97–137

Tiedtke M (1984) Sensitivity of the time-mean large-scale flow to cumulus convection in the ECMWF model. pp 297–316

Tiedtke M (1989) A comprehensive mass flux scheme for cumulusparameterization in large-scale models. Mon Weather Rev 117:1779–1800

Tokioka T (1988) The equatorial 30–60 day oscillation and the Arakawa–Schubert penetrative cumulus parameterization. J Meteorol Soc Jpn 66:883–901

Wang W, Schlesinger ME (1999) The dependence on convection parameterization of the tropical intraseasonal oscillation simulated by the UIUC 11-layer atmospheric GCM. J Clim 12:1423–1457

Webster PJ, Lukas R (1992) TOGA COARE: the coupled ocean-atmosphere response experiment. Bull Am Meteorol Soc 73:1377–1416

Wehner MF, Smith RL, Bala G, Duffy P (2010) The effect of horizontal resolution on simulation of very extreme US precipitation events in a global atmosphere model. Clim Dyn 34:241–247

Wilcox EM, Donner LJ (2007) The frequency of extreme rain events in satellite rain-rate estimates and an atmospheric general circulation model. J Clim 20:53–69